Turkish Journal of Electrical Engineering & Computer Sciences

http://journals.tubitak.gov.tr/elektrik/

Research Article

Turk J Elec Eng & Comp Sci
(2016) 24: 1223 – 1234

doi:10.3906/elk-1311-214

Ray tracing technique for shaping a dual reflector antenna system

Md. Rezwanul AHSAN[1,*], Mohammad Tariqul ISLAM[1], Yoshihide YAMADA[2], Norbahiah MISRAN[1]

[1]Department of Electrical, Electronic and Systems Engineering, Faculty of Engineering and Built Environment, Universiti Kebangsaan Malaysia, Bangi, Selangor, Malaysia

[2]Department of Electrical and Electronic Engineering, National Defense Academy, Yokosuka, Japan

Received: 26.11.2013 • **Accepted/Published Online:** 24.02.2014 • **Final Version:** 23.03.2016

Abstract: In radio astronomy applications, antennas having the highest aperture efficiencies are requested. In order to meet this request, a reflector shaping program for dual reflector antennas has been developed. The design procedure is based on the geometrical optics where differential equations have been formulated to define the ray trace of the antenna system. Recently, the fourth generation programming language MATLAB has become well known for its numerical computing environment and very useful three-dimensional data visualization functions. The authors wished to make a dual reflector shaping program by a ray tracing method in MATLAB. In this paper, details of the program are explained, and antenna ray tracing results are shown visually by three-dimensional viewgraphs. The numerical results are compared with the theoretical ones to confirm the correctness of the developed shaping program for a Cassegrain dual reflector antenna system. For uniform aperture distribution the first side lobe level is numerically obtained as –17.59 dB, which can be further reduced through shaping to –24.67 dB and –30.65 dB for parabolic and squared parabolic, respectively.

Key words: Ray tracing, geometrical optics, reflector antennas, dual reflector, reflector shaping, numerical analysis

1. Introduction

Dual reflector antennas have advantages over single reflector antennas because of their considerably higher directivity value and greater uniformity of radiation field distribution. Axial symmetric Cassegrain dual reflector antenna systems are the usual choice for high gain antenna applications in microwave and millimeter-wave bands [1]. These types of antenna system have relatively low, first sidelobes in all φ–cuts. The prime drawback of this system is the subreflector blockage, which is responsible for deteriorating the aperture efficiency. However, suitable modifications to the typical geometrical shape of the reflectors in the Cassegrain system can provide much higher efficiency with reduced spillover [2,3]. For achieving some particular specifications, i.e. antenna aperture efficiency, sidelobe levels, cross-polarization levels etc., both the main and subreflector need to be shaped accordingly.

The GO technique relies on the ray tracing method and is suitable for the design of reflectors if their dimensions are much larger than the wavelength. Throughout the design, a homogeneous surface has to be considered so that the produced ray paths are straight lines. One of the pioneering researchers, Galindo, first applied the GO technique for shaping the dual reflector system to achieve arbitrary phase and amplitude distributions over the main aperture [2]. The GO-shaping of reflector antennas has been achieved through simultaneous solution of partial differential equations (PDEs) that describe the ray trace system. The optimization basis of

*Correspondence: rezwanul.ahsan@yahoo.com

the PDE solution is the transformation of input wave to output wave by single reflection [4,5]. The formulation of differential equations for the shaping of reflectors has been described and applied to achieve desired aperture distribution [2,6,7]. The ray tracing method has also been employed to formulate nondifferential equations for shaping dual reflectors [8]. Other than solving PDE, an alternative method based on nonlinear algebraic equations derived using GO has been proposed for the shaping of dual reflectors and caustic lines [9,10]. However, for this kind of design, some approximations and assumptions need to be considered, which may suffer a slight variation in the shaping of the reflectors, which can be obtained by solving PDE through numerical analysis.

The shaping of a Cassegrain dual reflector antenna based on the ray tracing method is presented in this paper. In accordance with the desired aperture distribution and given uniform feed pattern, the formulation for differential equations has been generated considering the antenna's geometrical parameters. The simultaneous differential equations have been iteratively solved through numerical solutions using MATLAB, which gives the shaped profiles for both the main and subreflector. Some of the successfully employed design examples have been presented with their corresponding shaping, aperture distribution, and radiation pattern. Finally the accuracy of the designed program for shaping the dual reflector antenna system is ensured by comparing the numerical results with the theoretical results.

2. Geometry and structure of antenna

The coordinate system, antenna geometry, and structure are depicted in Figure 1 in cross-sectional view. The optical geometry of the dual reflector antenna consists of a hyperboloid subreflector between the paraboloidal main reflector and feed. The dual reflector antenna is of rotational symmetry around the Z-axis. The curved surfaces of the antenna system $M(z,x)$ represents the main reflector and $S(r,\theta)$ represents the subreflector.

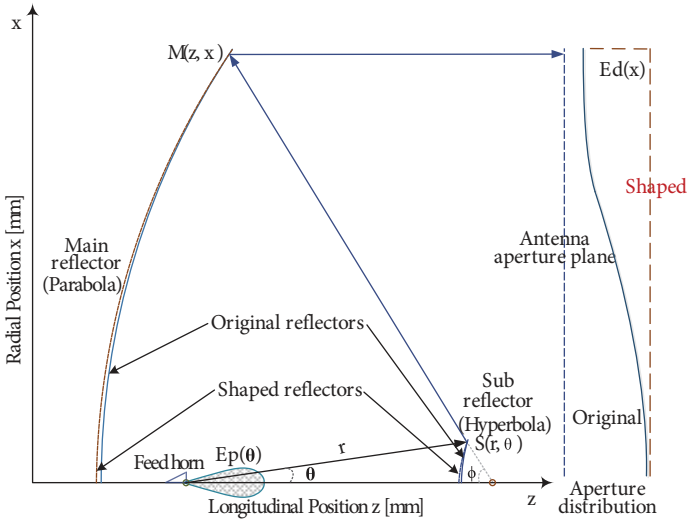

Figure 1. Geometry and structure of shaped dual reflector antenna.

A horn antenna is used as a uniform radiator with a radiation pattern as indicated by $E_p(\theta)$. For the design process, it is usual to choose a uniform feed horn pattern in achieving the solutions for numerical analysis. Typically it is considered that the feed horn would provide normalized peak illumination efficiency, i.e. 100% aperture efficiency, for analytical solution. In addition, an ideal, unrealizable feed antenna pattern would minimize the spherical scattering loss and abruptly reduce it to zero near the rim to avoid spillover. However, it has not yet been realized in practice. A practical feed is considered smaller than a few wavelengths in diameter

and has a wider pattern usually modeled with the $cos^q\theta$ pattern, where q is chosen to match the pattern of a real feed antenna at one point in addition to the unity beam peak [11–13]. After emitting from the feed horn, the ray is incident on the subreflector at an angle θ. The ray is then reflected and reaches the main reflector at an angle of φ. Finally, the ray is reflected from the main reflector and becomes parallel to the Z-axis. The front area of the main reflector and behind the subreflector is the aperture plane whose radiation pattern is given by $E_d(x)$. On the basis of aperture field distribution, the shaping of the reflector is determined by the ray tracing method. In this work, the initial functions for $E_p(\theta)$ and $E_d(x)$ are used given in the results section. Different aperture distributions and their corresponding shapes are obtained by changing the value of n ($n = 0, 1, 2$) in Eq. (12); a detailed explanation is presented in the Numerical Results and Discussion section.

3. Ray tracing technique for shaping a dual reflector antenna

3.1. Mathematics for ray tracing

The ray tracing method is based on the principle of GO, including Snell's law and conservation of energy, which are explained in this section. For the cases, the most significant rays are those directly from the sources and scattered rays from the reflected surface; the state of these rays provides the differential equations associated with GO for the shaping of both subreflector and main reflector surfaces. As we know from Snell's law, since the incident ray on the reflector and the surface normal vector are coplanar, the angle of indent and reflection are equal. The reflection conditions are graphically presented in Figure 2 for both a subreflector and main reflector surface. According to Snell's law, the following differential equation can be written for a subreflector surface (Figure 2a):

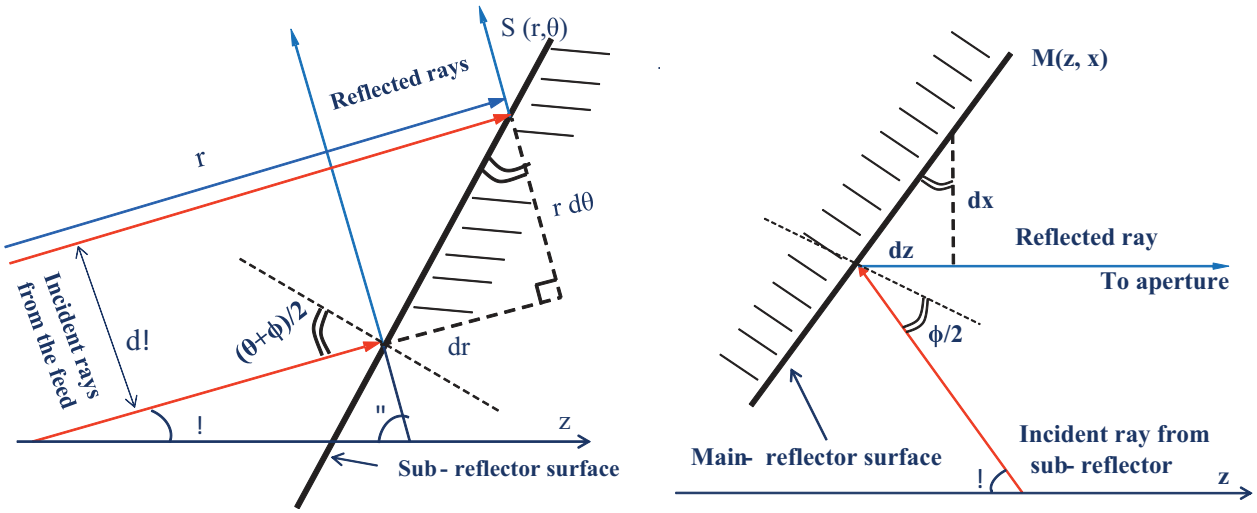

Figure 2. Detail of ray tracing (a) on subreflector surface (b) on main reflector surface.

$$\frac{dr}{d\theta} = r\tan\frac{\theta+\phi}{2} \tag{1}$$

In a similar way, the differential equation for a main reflector surface (Figure 2b) can be derived as follows:

$$\frac{dz}{d\theta} = \frac{dx}{d\theta}\tan\frac{\phi}{2} \tag{2}$$

According to the conservation of energy, the power radiated from the feed horn is required to be equal to the spread over energy on a circle normal to the reflected main beam in the aperture plane. The energy relation is presented in Figure 3 from which the energy conservation relation can be written as

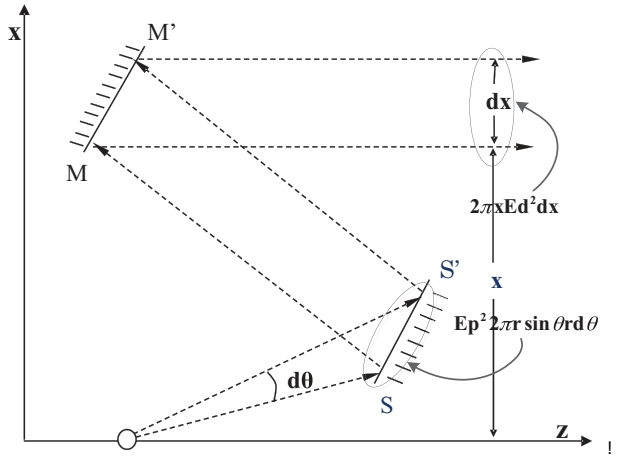

Figure 3. Energy relation.

$$E_p^2(2\pi r)\sin\theta r d\theta = 2\pi x E_d^2 dx \tag{3}$$

In Eq. (3), E_p^2 and E_d^2 should be normalized. For this purpose, the total energy conservation that is incident to the subreflector and distributed in the aperture is used [11,14]. The total energy conservation can be expressed by the following equation:

$$\int_0^{\theta_m} r^2 E_p^2 \sin\theta d\theta = \int_0^{x_m} x E_d^2 dx \tag{4}$$

In Eq. (4), r deviation in the left side integral is very small compared to the changes in E_p^2 as shown in Figure 1. Therefore, in the case of integration, r is the constant C.

$$C^2 \int_0^{\theta_m} E_p^2 \sin\theta d\theta = \int_0^{x_m} x E_d^2 dx \tag{5}$$

Through dividing Eq. (3) by Eq. (5), the normalization of E_p^2 and E_d^2 is achieved. Finally, the next differential equation is obtained.

$$\frac{dx}{d\theta} = \frac{E_p^2(\frac{r}{c})^2 \int\limits_0^{x_m} E_d^2 x dx}{x E_d^2 \int\limits_0^{\theta_m} E_p^2 \sin\theta d\theta} \tag{6}$$

For the design process, the horn radiation pattern $E_p(\theta)$ and the aperture distribution $E_d(x)$ are given to achieve the desired radiation characteristics. Using the known values of $E_p(\theta)$ and $E_d(x)$, the value of $dx/d\theta$ is determined with Eq. (6). The function $dx/d\theta$ is then substituted into Eq. (2) and Eq. (1), which gives a simultaneous differential equation. By repeating the steps of computation through numerical solutions of the simultaneous differential equation, finally the shaping profiles for the main reflector and subreflector are achieved.

3.2. Calculating the radiation patterns

The direction of travel of the plane wave is along the z-axis as presented in Figure 4 and the radiation patterns are calculated using the theoretical aspects presented in [12] and [11]. Considering the aperture surface in the $x--y$ plane of the aperture plane, the radiated electromagnetic wave Er can be expressed as

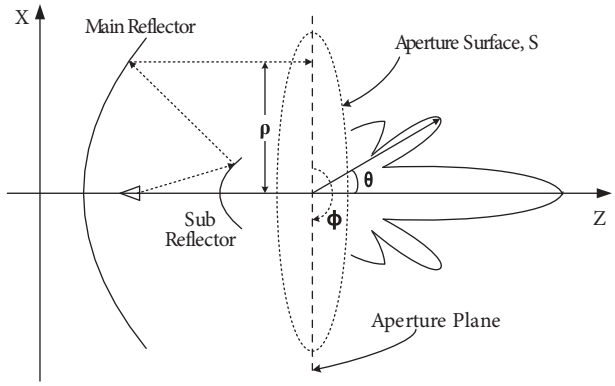

Figure 4. Radiation characteristic of Cassegrain antenna system.

$$E_r = \frac{j\exp(-jkR)}{R}\iint\limits_S E_d(x,y)\exp[jk\sin\theta(x\cos\phi + y\sin\phi)]dxdy \tag{7}$$

More specifically we can write

$$F(\theta,\phi) = \frac{1}{S}\iint\limits_S E_d(x,y)\exp[jk\sin\theta(x\cos\phi + y\sin\phi)]dxdy \tag{8}$$

where $k = 2\pi/\lambda$

Eq. (8) represents the Fourier integral transform of electric field strength and for a rotational symmetric Cassegrain antenna we can consider

$$\begin{aligned} x &= \rho\cos\phi \\ y &= \rho\sin\phi \end{aligned} \tag{9}$$

Using Eq. (8), the generalized form for the radiation field can be achieved:

$$\begin{aligned} F(x,\phi^{'}) &= \frac{1}{S}\int_0^{2x}\int_0^{D/2} E_d(x)\exp[jkx\sin\theta(\cos\phi\cos\phi^{'} + \sin\phi\sin\phi^{'})]xdxd\phi^{'} \\ &= \frac{1}{S}\int_0^{2x}\int_0^{D/2} E_d(x)\exp[jkx\sin\theta(\cos(\phi-\phi^{'}))]xdxd\phi^{'} \\ F(x) &= \frac{4}{\pi D^2}2\pi\int_0^{x_m} E_d(x)J_0(k\rho\sin\theta)xdx \end{aligned} \tag{10}$$

Due to the direction in which the wave front progresses, *(1+cos θ)/2=cos2(θ /2)* is the obliquity factor and the radiation directivity, $D(x)$, can be expressed as

$$\begin{aligned} D(x) &= D_0[(\tfrac{1+\cos\theta}{2})F(x)]^2 \\ &= D_0[\cos^2\tfrac{\theta}{2}F(x)]^2 \end{aligned}, \tag{11}$$

where $D_0 = jexp(-jkx_m)/x_m$.

4. Numerical results and discussion

Following the flow diagram as depicted in Figure 5, a MATLAB program has been coded to validate the ray tracing method for the shaping scheme of the Cassegrain type dual reflector system. By giving the initial values of antenna parameters, the program will produce the reflectors' shaping as per the requirement. An example of a design is presented here with the following parameters: main reflector radius $Rm = 2$ m, subreflector radius $R_s = 0.2$ m, maximum aperture angle $\varphi_m = 75^\circ$, main reflector focal length $f_m = 1.3$ m, feed to focus length $a = 0.5$ m, subreflector angle $\theta_f = 26.61^\circ$, frequency 3 GHz. The ray tracing method has been successfully applied to calculate profiles for reflectors shape, ray lengths to the aperture, aperture distribution, and radiation patterns.

4.1. Aperture distribution and reflector shapes

The designed subreflector and main reflector shapes are presented in Figure 6 with their corresponding aperture distributions presented in Figure 7. For this work, the following initial functions are used for $E_p(\theta)$ and $E_d(x)$:

$$\begin{aligned} E_p^2(\theta) &= (\cos\theta)^{epn}; \quad \text{where } epn = 7.8662381 * 2 \\ E_d^2(x) &= \left[1 - \left(\frac{x}{x_{\max}}\right)^2\right]^n; \quad \text{where } n = 0,\ 1,\ 2 \end{aligned} \tag{12}$$

Here the values of n determine the aperture distribution type through tapering for several circular apertures. The tabulated data (Table 1) show the properties of common circular aperture tapers and aperture distribution for different values of n [12]. The value $n = 1$ gives a parabolic distribution, in which case a smooth taper is observed from the center of the aperture to the edge where aperture field is zero. A unity aperture efficiency is achieved for $n = 0$; the distribution becomes uniform throughout the circular aperture. Compared to the uniform distribution, the parabolic taper ($n = 1$) provides lower side lobes with the cost of wider beamwidth and reduced directivity. This effect is more noticeable for the parabolic squared ($n = 2$) distribution if further reduction of side lobs is required for specific applications.

4.2. Ray tracing

The reflector shapes as shown in Figure 7 change the caustic line to distribute the power accordingly. For accuracy, a reasonable number of surface points are created and investigated. Figure 8 shows how the reflection of rays occurs for different shaped surfaces (uniform, parabolic, and parabolic squared, respectively). It is considered that the end points of the shaped subreflector lie on the reference hyperboloid rim (for $n = 0$, uniform). The z-axis crossing points of the shaped subreflector is moved toward the main reflector, anticipating the steeper slope of the shaped surface that results in delivering most of the power from the feed horn near

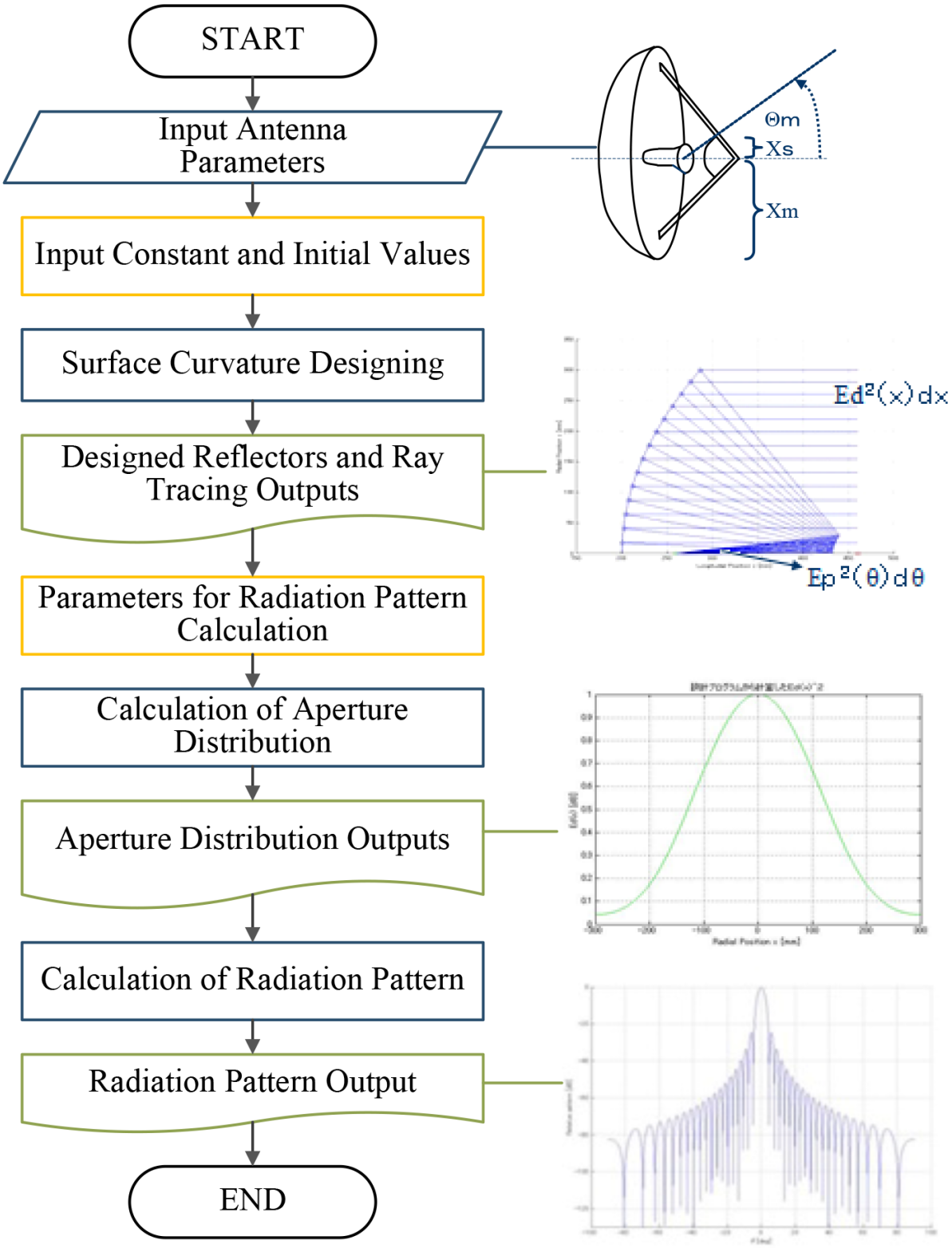

Figure 5. Flow diagram of the shaping dual reflector antenna system.

the axis, which resembles the outer portion of the aperture up to a power density equal to the central portion. Figure 9 presents different stages of 3-D ray tracing for uniform aperture distribution.

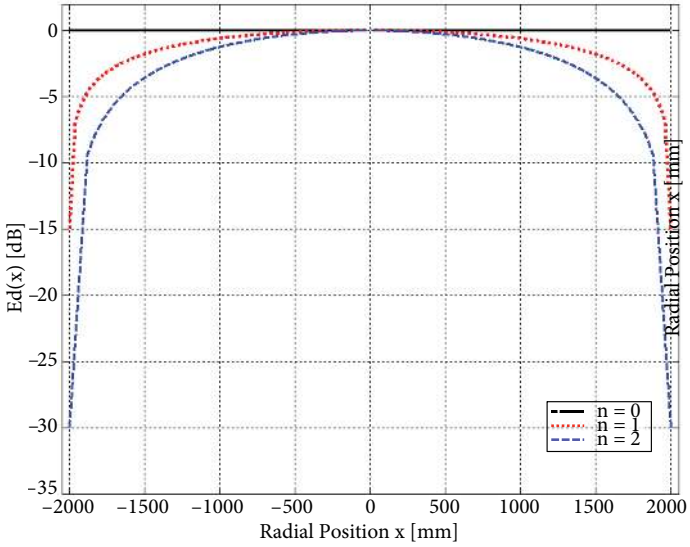

Figure 6. Aperture distribution for dual reflector antenna system.

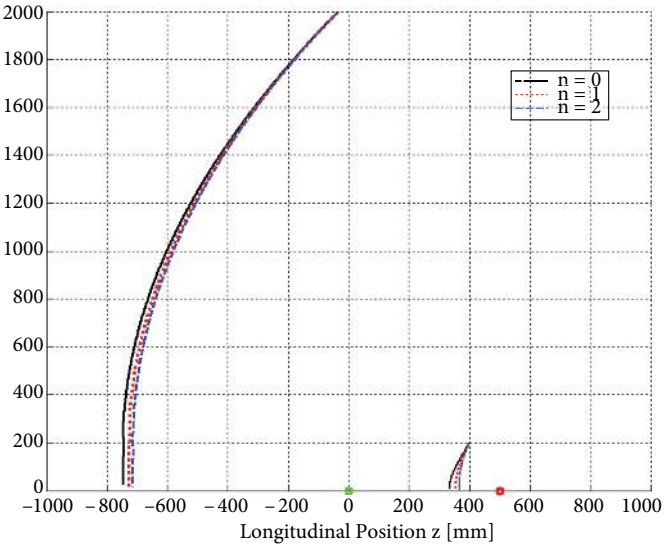

Figure 7. Designed main reflector and subreflector shapes.

Table 1. Characteristics of parabolic taper.

n	Half power (rad)	Side lobe level (dB)	Aperture distribution
0	$1.02\lambda/2\ x_{max}$	−17.6	Uniform
1	$1.27\ \lambda\ /2\ x_{max}$	−24.6	Parabolic
2	$1.47\ \lambda/2x_{max}$	−30.6	Parabolic Squared

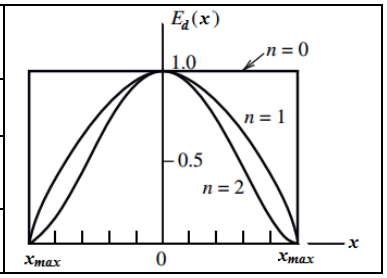

***Book: Antenna Theory and Design, Stutzman and Thiele 3rd Ed., Pg. 389, Table 9-2a.

4.3. Radiation patterns

With the given aperture distribution, tracing rays from the feed to the aperture can be set up and integrated to obtain the far-field distribution. The ray tracing technique is used to calculate the aperture field distribution and the far-field radiation patterns are determined through Eq. (10). The formulation associated with the ray tracing method for uniform aperture phase distribution produces a symmetric pattern due to the property of the Fourier transform [9,10,12]. The Cartesian forms of normalized radiation patterns for different aperture distributions are presented in Figure 10. The figure exhibits the radiation patterns for different aperture tapers, which are presented to validate the accuracy of the method implemented in MATLAB. The accuracy of the designed program is determined by comparing the results with the theoretical ones. To conclude the analysis and for comparison, the process related to deducing and presenting the radiation patterns is considered as found through a literature review [3,5,10–12].

It has been observed that, in comparison to uniform distribution ($n = 0$), the shaped reflectors become more directive with the increase in θ and side lobe levels decrease accordingly for corresponding subreflector

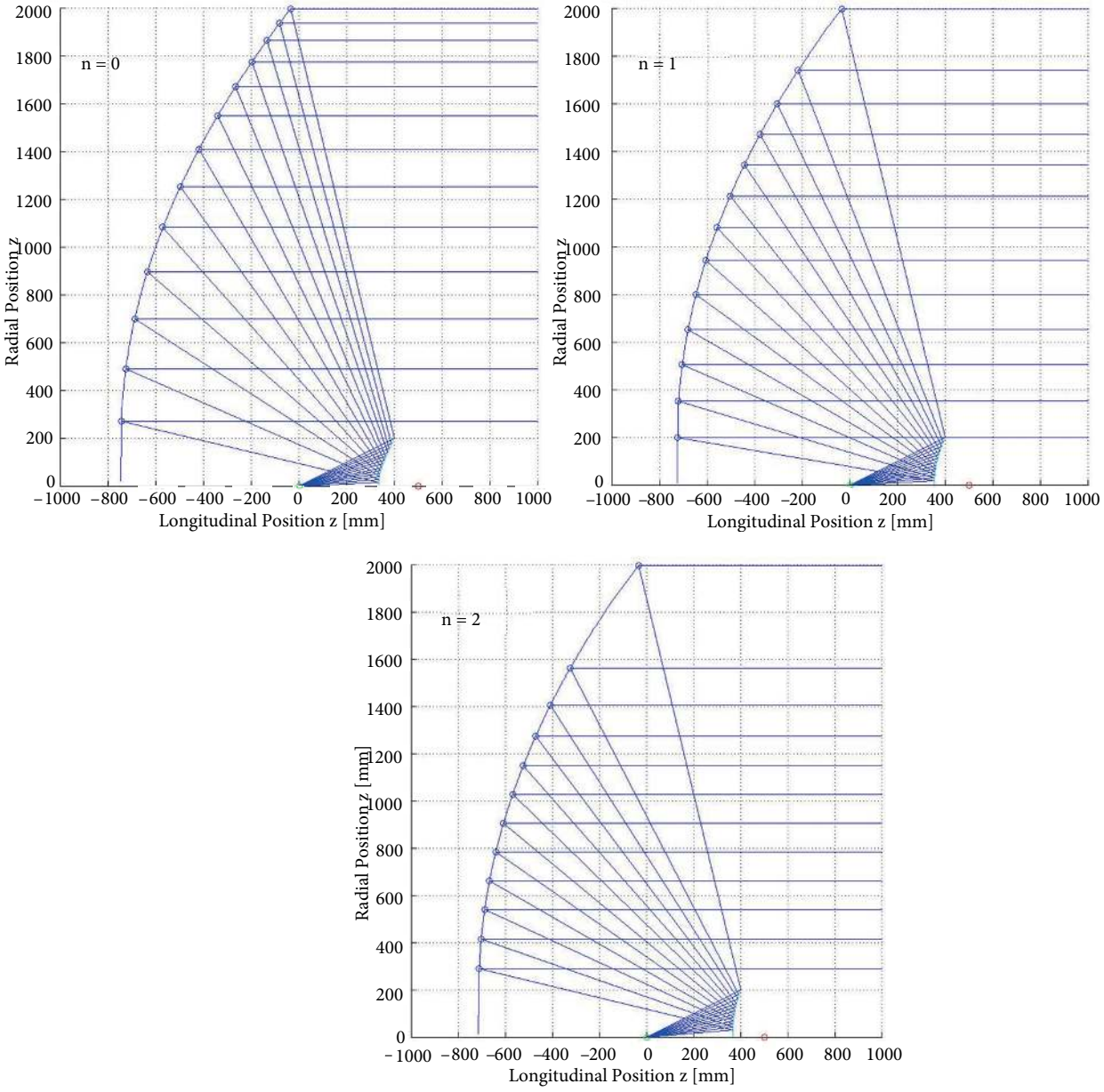

Figure 8. 2-D ray tracing for n = 0 (uniform), 1 (parabolic), 2 (parabolic squared).

illumination and the main reflector radiation for the axis symmetry region takes up with main reflector's surface diffraction as the main reflector is illuminated by the reflected power from the subreflector. The shaping of the both the reflector surfaces greatly affects the radiation patterns. The accuracy of the shaping of the dual reflector antenna can be easily identified by comparing the theoretical value [12] for the half power beam width (HPBW) and side lobe level (SLL) with the achieved results after shaping the reflector surfaces. Tabular data are presented for this purpose in Table 2. For the case of uniform aperture distribution, the first SLL can be observed at –17.59 dB and lower side lobe levels keep decreasing with the increase in θ. However, for shaped reflector surfaces the first SLL can be seen at –24.67 dB and –30.65 dB, respectively, and next side lobe levels are decreasing greatly. The shaping of the reflector surfaces makes it possible to concentrate most of the reflected

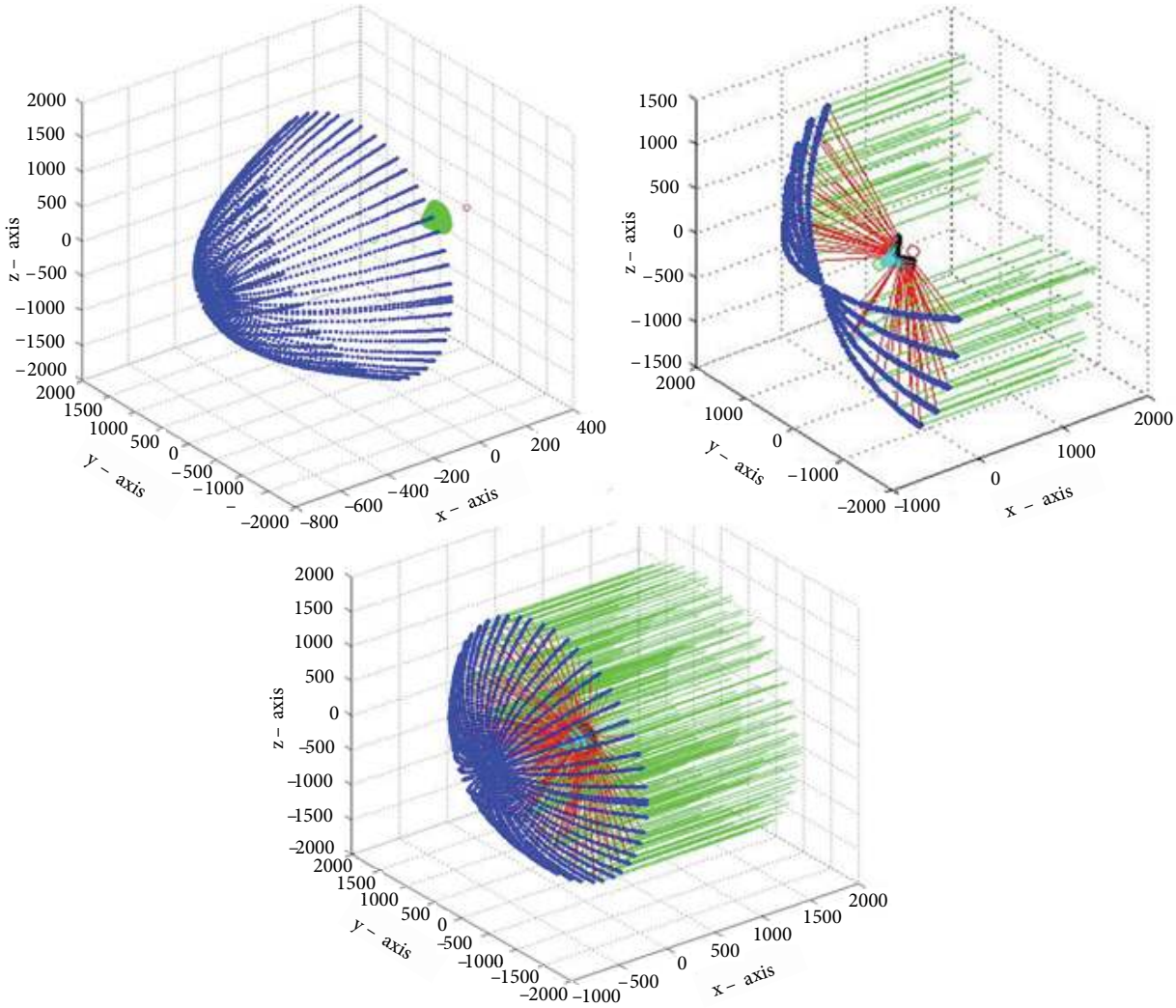

Figure 9. 3-D shaping and ray tracing for uniform aperture distribution.

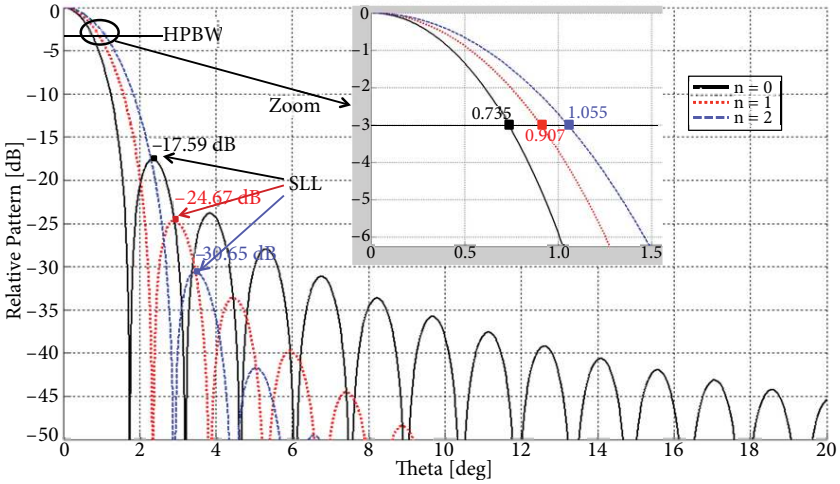

Figure 10. Radiation for shaped dual reflector, $n = 0, 1, 2$.

and radiated energy near the axisymmetric center of the surfaces and further reduces the effective distance from the surface; they are collectively responsible for achieving the greatly decreased side lobe levels.

Table 2. Comparison between theoretical and achieved results.

	Half power (rad)		Side lobe level (dB)	
n	Theoretical	Achieved	Theoretical	Achieved
0	0.02550	0.02569	–17.6	–17.59
1	0.03175	0.03168	–24.6	–24.67
2	0.03675	0.03683	–30.6	–30.65

5. Conclusion

This paper discusses the shaping procedure of a Cassegrain dual reflector antenna designed and the program developed in the MATLAB programming environment. The design procedure of the shaping program is carried out through the formulation of differential equations for geometrical configuration of the dual reflector antenna. The ray tracing/GO algorithm is employed for developing the interrelated equations for the geometrical surface of both reflectors and solving them through numerical synthesizing. Some usual constraints are applicable for the GO technique like homogeneous space, uniform phase across the aperture, Snell's law, energy conservation law, and equal physical path length for each ray to reach the aperture plane from the feed point. Since the functions of the numerical solution from MATLAB are used in solving the simultaneous differential equations, errors are assumed to be negligible for obtaining profiles for shaped reflectors. However, the errors can be reduced by narrowing down the quantization grid for the reflector surface, which is considered at initialization state. The processing time will be certainly increased considerably to provide a fine solution for profiles of both reflector surfaces. Usefulness of the developed program is ensured through designing reflector surfaces for different aperture distributions. The comparison results in terms of HPBW and SLL between the theoretical and numerical are placed in a table. Investigating the numerical results it can be concluded that the developed program module for shaping a Cassegrain dual reflector has been done successfully through the ray tracing technique. To fulfil the requested design for given aperture distribution and feed pattern, the shaping program can successfully be employed in designing the Cassegrain dual reflector antenna system.

Acknowledgments

The authors would like to acknowledge the support from UKM Research University Grant - DIP-2012-006 (Dana Impak Perdana) and National Defense Academy, Japan.

References

[1] Sletten CJ. Reflector and Lens Antennas: Analysis and Design Using Personal Computers. 1st ed. Norwood, MA, USA: Artech House, 1988.

[2] Galindo V. Design of dual-reflector antennas with arbitrary phase and amplitude distributions. IEEE T Antennas Propag 1964; 12: 403-408.

[3] Collins GW. Shaping of subreflectors in Cassegrain antennas for maximum aperture efficiency. IEEE T Antennas Propag 1973; 21: 309-313.

[4] Williams WF. High efficiency antenna reflector. Microw J 1965; 8: 79-82.

[5] Baker L. Reflector shaping by optimization of wavefront shapes. In: International Symposium on Antennas and Propagation Society; 24–28 June 1991; Ontario, Canada: IEEE. pp. 172-174.

[6] Kinber BY. On two-reflector antennas. Radio Eng Electron Phys 1962; 6: 914-921.

[7] Moreira FJS, Prata Jr. A, Bergmann JR. GO shaping of omnidirectional dual-reflector antennas for maximum gain. In: SBMO/IEEE MTT-S International Conference on Microwave and Optoelectronics; 25–28 July 2005; Brasilia, Brazil: IEEE. pp. 665-668.

[8] Kildal PS. Synthesis of multireflector antennas by kinematic and dynamic ray tracing. IEEE T Antennas Propag 1990; 38: 1587-1599.

[9] Kim Y, Lee TH. A new shaping method for circularly symmetric dual reflector antennas. In: IEEE International Symposium on Antennas and Propagation Society; 3–8 July 2005; Washington, USA: IEEE. pp. 470-473.

[10] Moreira FJS, Jose RB. Shaping axis-symmetric dual-reflector antennas by combining conic sections. IEEE T Antennas Propag 2011; 59: 1042-1046.

[11] Lo YT, Lee SW. Antenna Handbook: Antenna Theory, 1st ed. Berlin, Germany: Springer-Verlag, 1993.

[12] Stutzman WL, Thiele GA. Antenna Theory and Design, 3rd ed. Hoboken, NJ, USA: John Wiley & Sons, 2012.

[13] Balanis CA. Modern Antenna Handbook. Hoboken, NJ, USA: John Wiley & Sons, 2011.

[14] Lee J, Parad L, Chu R. A shaped offset-fed dual-reflector antenna. IEEE T Antennas Propag 1979; 27: 165-171.